Double-average mean flow and local turbulence intensity profiles from PIV measurements for an open channel flow with rigid vegetation

R. Martino, A. Paterson & M. Piva

Environmental Fluid Mechanics

ISSN 1567-7419
Volume 12
Number 1

Environ Fluid Mech (2012) 12:45-62
DOI 10.1007/s10652-011-9221-4

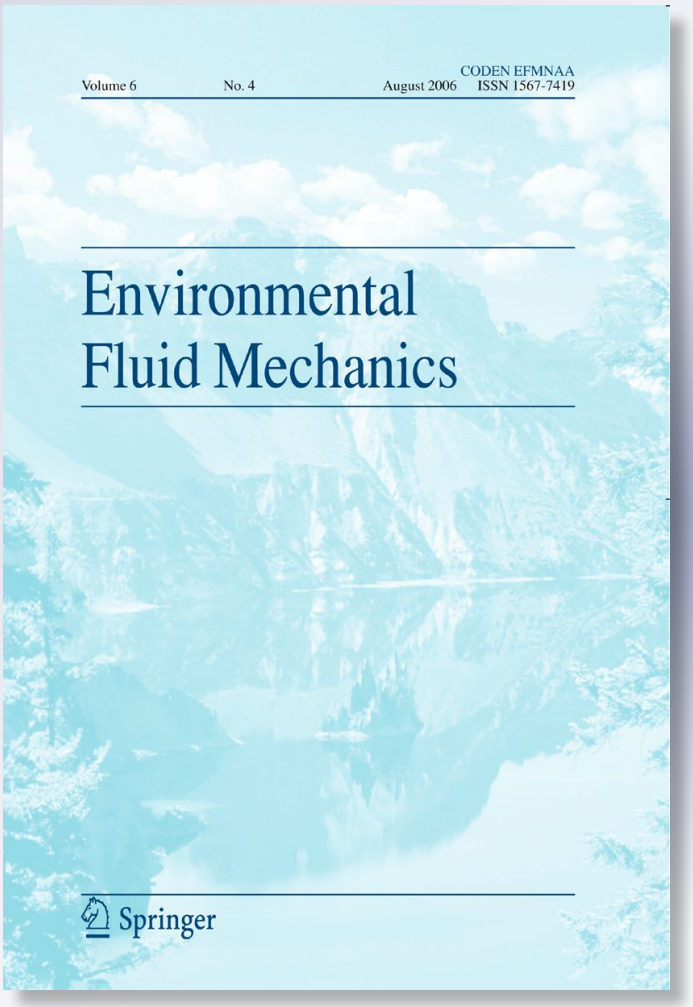

Springer

Environ Fluid Mech (2012) 12:45–62
DOI 10.1007/s10652-011-9221-4

ORIGINAL ARTICLE

Double-average mean flow and local turbulence intensity profiles from PIV measurements for an open channel flow with rigid vegetation

R. Martino · A. Paterson · M. Piva

Received: 2 September 2010 / Accepted: 12 September 2011 / Published online: 28 September 2011

Abstract This contribution presents particle image velocimetry measurements for an open channel stationary uniform and fully developed flow of water over a horizontal flat bed of uniform glass beads in presence of a staggered array of vertical cylindrical stems. The main objective was to explore and quantify the influence of the stems-to-flow relative submergence, h_v/h, over the mean flow and local turbulence intensities. A comparison with measurements for the non-vegetated flow over the same granular bed is presented. Results indicate a remarkable influence of h_v/h over the whole flow field. The time-average mean flow presents a strong spatial variation in the layer of the flow occupied by the stems. The local velocity fluctuations are strongly affected by the presence of the stems, with regions in between the stems where they reach peaks that are several times larger than those encountered in the flow in absence of vegetation. The turbulence intensity profiles are noticeably different when compared to those measured in the non-vegetated flow conditions. From previous works it was possible to derive an equation for the mean velocity, U_v, of the flow through the vegetated layer of height h_v. The prediction of this equation is in good agreement with the uniform value for the double-average longitudinal velocity profile in this layer. A final brief discussion about the possible impact of these vegetated-flow features on the sediment transport is presented.

Keywords Vegetated flow · Double-averaged velocity profiles · Turbulence level · PIV technique

R. Martino (✉) · M. Piva
Grupo de Medios Porosos, Facultad de Ingeniería, Universidad de Buenos Aires,
Paseo Colón 850, 1063 Buenos Aires, Argentina
e-mail: rmartino@fi.uba.ar

A. Paterson
Departamento de Hidráulica, Facultad de Ingeniería, Universidad de Buenos Aires,
Las Heras 2214, 1127 Buenos Aires, Argentina

1 Introduction

The need to mitigate and protect the soil from erosion processes, as well as programming the sustainable management of wetlands, flood plains and large river ecosystems is now a major challenge for engineers, biologists and ecologists. However, most of the relevant hydraulic and sedimentary processes arising from the coupling between flow, sediment and vegetation, are not yet fully understood [1–3].

In general, vegetation increases flow resistance, substantially alters the turbulence of the flow field and modifies the transport and deposition of solids, nutrients and contaminants [4–6]. This influence has not yet been adequately incorporated into the hydraulic design and modelling because of the complexity of the many variables that govern the phenomenon. In particular, it is not fully clarified what spatial and temporal scales of the flow should be investigated.

Vortices and eddies of various length scales arise from the interaction between walls or solid objects and the flow field. Trying to represent these flow characteristics in detail is a huge task. The classical formulae [7], arising from height-averaged quantities and scaling considerations, give a description for the bulk mean flow. However, if the size of the irregularities or the height of the resistance elements are of the same order of magnitude as the flow depth, available methods are no longer valid [7–9]. This is the case of flows in the presence of rigid stems, which are considered a first step in understanding the global phenomenon of vegetated flows [10].

The works of Carollo [11] and Poggi [12] have pointed out the importance, not only for the mean flow in the vegetated layer but also over it, of the number of stems per unit area of the bed or stems density, m, which is mainly related with the mean distance between stems, a. Huthoff [13] and Baptist [14] explicitly include this variable in their models for the analysis of the mean flow in presence of rigid vegetation.

Stone and Shen [10] gave an explicit expression for the total resistance on the flow as the sum of two contributions, one due to bed roughness and the other arising from the hydrodynamic drag force on the stems. They showed that the bed contribution is affected by the term $(1 - \lambda_S)$, where λ_S, defined as $\lambda_S = m\pi d_v^2/4$, being d_v the stems diameter, is the solidity of the stems matrix. On the other hand, the stems resistance depends on $\lambda_K = mh_v d_v$, with h_v the vegetation height, the frontal area of the stems as seen by the incident flow.

The work of Nepf [15] showed that the stems-to-flow relative submergence, h_v/h, being h the total flow depth, separates very different flow regimes, ranging from well submerged ($h_v \ll h$) to emergent vegetation ($h_v = h$).

The present work reports measurements of the velocity flow field obtained with particle image velocimetry (PIV) in a small horizontal open channel in presence of a staggered distribution of rigid stems over a rough bed of glass beads. The main objective was to explore the influence of h_v/h on the flow field features in the whole flow depth, h, along the longitudinal distance between two consecutive stems, as representative of a basic flow cell for the regular array of stems.

This paper is structured as follows: Sect. 2 presents a brief state-of-the-art discussion, Sect. 3 describes the channel setup, Sect. 4 is devoted to present the PIV non-intrusive velocimetry technique, Sect. 5 presents the measurements with the analysis and discussion, and finally in Sect. 6 there are the main conclusions and perspectives.

2 State of the art

Rigid vegetation can be thought as a large scale roughness superimposed to the granular bed roughness [7,8]. Because of the complexity of the whole phenomenon, the problem of getting a complete description of this perturbed flow is still open [14].

Among the most important questions that have no definitive answer we can mention those related to the sources of turbulence production, the size of the turbulent eddies and its interactions [12,13,15]. For example, several hypothesis have been proposed in order to describe and to model the intense shear layer at the top of the canopy that separates the flow inside the vegetation layer from the free flow over the plants [13,16].

The possibility to adjust analytical expressions (logarithmic, hyperbolic tangent) to the mean flow velocity profiles depends on the definition of appropriate length and velocity scales, and, again, the discussion does not have a complete closure [11,15].

Mean flow velocity for stationary uniform conditions over rough beds, $\bar{U} = Q/(bh)$, being Q the flow rate, b the channel width and h the flow depth, can be computed in terms of the slope, i, and the hydraulic radius, R, using the Chezy coefficient, C [7]:

$$Q/(bh) = C\sqrt{Ri} \approx C\sqrt{hi} \tag{1}$$

where it has been assumed that R is close to h. The recent work of Baptist [14] gives an expression for C for flows in presence of rigid stems, valid for $h_v \leq h$:

$$C = \sqrt{\frac{1}{\frac{1}{C_b^2} + \frac{C_{Dv} m d_v h_v}{2g}}} + \frac{\sqrt{g}}{\kappa} \ln\left[\frac{h}{h_v}\right] \tag{2}$$

where $\kappa = 0.41$ is the Von-Karman constant, C_{Dv} is the drag stem coefficient and C_b is the granular bed Chezy coefficient, related with the Darcy–Weisbach–Colebrook coefficient, f_b, or the Strickler coefficient, f_S, by [7]:

$$C_b^2 = \frac{8g}{f_b} = \frac{g}{f_S} \tag{3}$$

It is also usual to perform a control volume analysis, extended to the entire flow depth, for the balance of momentum in the longitudinal direction of the stream, based on the two-layer approach for the flow in presence of rigid stems, under the assumptions of steady and uniform flow, see for example Huthoff [13]. From this analysis it can be deduced an expression for the depth-averaged mean flow velocity inside the region occupied by the stems, U_v:

$$U_v = \sqrt{\frac{ghi}{f_S + \frac{C_{Dv} m d_v h_v}{2}}} \tag{4}$$

valid for $h_v \leq h$, as can be verified by replacing $h_v = h$ in the last equation to recover Eq. 5 of the quoted work.

Based on the above expressions, an equation relating U_v with $\bar{U} = Q/(bh)$ can be derived. Let us begin by replacing Eq. 2 in Eq. 1:

$$Q/(bh) = \left\{\sqrt{\frac{1}{\frac{f_b}{8} + \frac{C_{Dv} m d_v h_v}{2}}} + \frac{1}{\kappa} \ln\left[\frac{h}{h_v}\right]\right\} \sqrt{ghi} \tag{5}$$

where the relationship between f_S and f_b, given by Eq. 3, has been used. Then, by replacing $\sqrt{ghi}$ in terms of U_v as given by Eq. 4, it is obtained:

$$Q/(bh) = \left\{ \sqrt{\frac{1}{\frac{f_b}{8} + \frac{C_{Dv} m d_v h_v}{2}}} + \frac{1}{\kappa} \ln\left[\frac{h}{h_v}\right] \right\} \sqrt{\frac{f_b}{8} + \frac{C_{Dv} m d_v h_v}{2}} U_v \tag{6}$$

an, finally, after some algebra, it can be deduced the following equation:

$$U_v = \frac{\frac{Q}{bh}}{\left[1 + \frac{1}{\kappa}\sqrt{\frac{f_b}{8} + \frac{C_{Dv}\lambda_K}{2}} \ln\left[\frac{h}{h_v}\right]\right]} \tag{7}$$

Equation 7 shows that U_v is proportional to $\bar{U}$ affected by a coefficient which combines the effects of the main sources of flow resistance: the granular bed roughness and the hydrodynamic drag on the stems. When $h_v = h$ (emergent stems) it follows that $U_v = \bar{U}$. On the other hand, if $h_v < h$ (submerged stems), $\ln(h/h_v) > 0$ and, therefore, the total resistance coefficient can adopt values larger than one, depending on λ_K. Thus, an array of very dense but thin stems can offer a restriction to the flow similar to that offered by a sparse array of stems with a larger diameter.

Regarding the value for the stems drag coefficient, Stone and Shen [10] reported $C_{Dv} = 1.05$ for a wide range of diameters, heights and densities. Moreover, they present a compilation of experimental values measured by other researchers, from which it is possible to infer an uncertainty $\Delta C_{Dv} = 0.08$ for m ranging between 100 and 2,500 stems/m^2 and stems diameters d_v between 0.15 and 1.27 cm. The (unpublished) measurements of Meijer [38], as can be found in Klopstra [17], confirm this result: they report eight experiments combining different flow rates over an array of metallic cylinders with 8 mm uniform diameter, with $0.91 \leq C_{Dv} \leq 1.18$. García et al. [18] have reported that in an open channel lined with rigid cylinders, the bulk drag coefficient is $C_{Dv} = 1.13 \pm 0.18$. It has been assumed that the C_{Dv} is the same for both emergent and submerged stems conditions. This is a reasonable assumption if the stem aspect ratio $h_v/d_v \geq 5$ because if $h_v/d_v < 5$ a change has been found in the wake structure [13].

While the quoted works state that the bed roughness term in the quantification of U_v is negligible when compared with the stems resistance term, it will be included for completeness using the relationship for fully developed rough flow [7,13,19]:

$$\frac{f_b}{8} = f_S = \frac{1}{64}\left[\frac{k d_s}{h}\right]^{1/3} \tag{8}$$

with $k \approx 2.5$ for a flat bed of uniform glass beads [4,7].

We note that an estimation of the velocities in the vegetated zone for known Q and h is useful in cases where the density of the vegetation does not allows the introduction of instruments used in field measurements (ADV, current meters). Even in those cases where the instruments penetrates the vegetated layer, reference values should be provided to set the instruments. In particular, in the present work, the result of Eq. 7 was useful to set the measurement parameters during the implementation stage of the PIV technique.

3 Channel facilities

The measurements were performed in a small 4.00 m long and 15 cm width horizontal open channel with transparent Plexiglas walls. A mean flow $\bar{U} = Q/(bh) = 6.0$ cm/s with

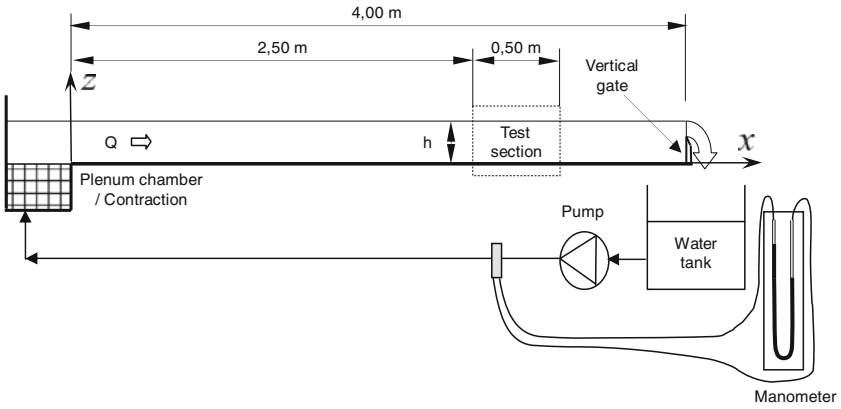

Fig. 1 Scheme of the small horizontal channel and the equipment used for driving a 4.0 cm depth flow, with $\bar{U} = 6.0$ cm/s (scheme is not drawn to scale)

constant depth, $h = 4.0$ cm, was imposed with a centrifugal pump. The flow depth was controlled with a vertical gate at the flow exit, and was measured with transparent millimeter rulers fixed at the channel wall along four stations (1.20, 2.20, 2.80 and 3.00 m from the flow inlet).

Temperature of the fluid was registered in order to have actual water density, ρ, and viscosity, μ. In all runs the flow Reynolds number, $Re = \bar{U} D_h / \nu$, were D_h is the channel hydraulic diameter and ν the kinematic viscosity, was kept to a constant value of 6,300.

The Reynolds number and the flow depth, were kept constant in order to study the influence of the relative submergence on the structure of the flow velocity field. On one hand it is desirable a high value for the width-to-depth ratio of the channel for generating close to two-dimensional flow. But, on the other hand, it is necessary to have a reasonable flow depth that allow to explore the largest possible range of the ratio h_v/h. The chosen depth $h = 4$ cm takes into account these two restrictions. The Reynolds number of about 6,300 (based on the hydraulic diameter of the channel) allowed simultaneously to impose a turbulent flow in the test section without exceeding the maximum velocity of the flow that our instruments are able to measure.

Prior to entering the channel, the flow was driven through a plenum chamber and a converging section. The test section was located 2.50 m from the flow inlet. See Fig. 1 for more details.

A layer of 1.00 m of crushed rocks with an averaged size of about 1.0 cm was placed along the bed from the flow inlet, in order to get a rapid transition to turbulent rough flow conditions [12,15]. After this initial rough layer the bed was composed by a 2.00 m long flat layer of uniform glass-beads of density 2.65 g/cm^3 and mean diameter $d_s = 0.63 \pm 0.09$ mm. Figure 2 shows the test section of the channel with $h_v = 2.8$ cm, in which it can be observed the flat granular bed and the free surface of the flow with the meniscus over the transparent channel wall.

The rigid vegetation are vertical cylindrical rods of bronze, with diameter $d_v = 2.00 \pm 0.02$ mm. They were inserted into the orifices of a metallic frame below the granular bed in a staggered array, see Fig. 2. This configuration of rigid vegetation was used by Stone and Shen [10] in their experimental work. With a distance between stems of 17.5 mm results array of density $m = 3,770$ stems/m^2 and solidity $\lambda_S = 0.03$. The height of these rigid stems, h_v, was varied from 0.5 to 4.0 cm decreasing the thickness of the sediment layer from 5.5 to 2.0 cm, covering the range of the relative submergence, h_v/h, from well submerged to emergent vegetation.

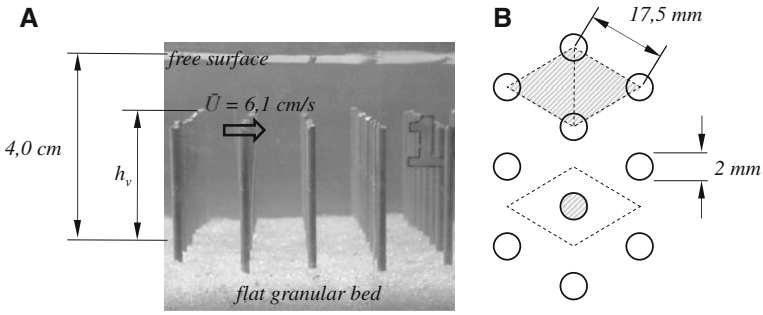

Fig. 2 The channel test section: **a** picture of the flat granular bed of uniform glass beads with rigid staggered vegetation; **b** scheme of the main dimensions of the cylindrical stems array

It is emphasized that measurements without stems, over the same granular flat bed, were previously taken in order to get a direct comparison of the influence of the stems array over the flow.

4 The PIV technique

The PIV technique is based on the correlation between two consecutive images of tracer particles in a selected plane of the flow. The pair of images under analysis are separated by a known time span. The technique is statistical in the sense that we are not interested in the evolution with the flow of every single particle but on the motion of particle patterns.

The images are subdivided in small interrogation windows, over which the correlation function is sequentially computed. The position of the correlation peak on each window is the displacement vector, $\Delta\mathbf{d}$, for the particle pattern in this portion of the image. Dividing $\Delta\mathbf{d}$ by the time interval between the two consecutive images under analysis, Δt, results the velocity vector for the point associated with the central point of every interrogation window, until covering the complete image recorded. More details can be found in Raffel [20], Adrian [21–23], Prasad [24] and the Measurement Science and Technology series of articles devoted to this technique [25–30].

The flow was expected to be fully developed, stationary, uniform and turbulent, even for the case without stems. The injection of dye allowed for a qualitative previews of the flow, showing a highly three-dimensional turbulent flow with recirculation zones immediately downstream of the stems. The uniform distribution of the dye in the bulk of the flow at a short distance from the injection point indicated a strong turbulent mixing in the vegetated flow. All these features were reported in previous works [11–13,15].

The PIV technique was applied mounting a continuous laser-sheet Nd-Yag of 10 mW at 530 nm orthogonal to a CCD monochrome camera PixeLINK A-741, see Fig. 3. The camera was connected to a FireWire IEEE 1391 PC frame grabber.

The flow was seeded with tracer polyamide particles of diameter $d_{piv} = 50\,\mu$m and density $\rho_{piv} = 1.03\,\text{g/cm}^3$ (www.dantec.com). Under the hypothesis of motion in the Stokes regime, final velocity is [31]:

$$u_\infty = \frac{g d_{piv}^2 (\rho_{piv} - \rho)}{18\mu}. \tag{9}$$

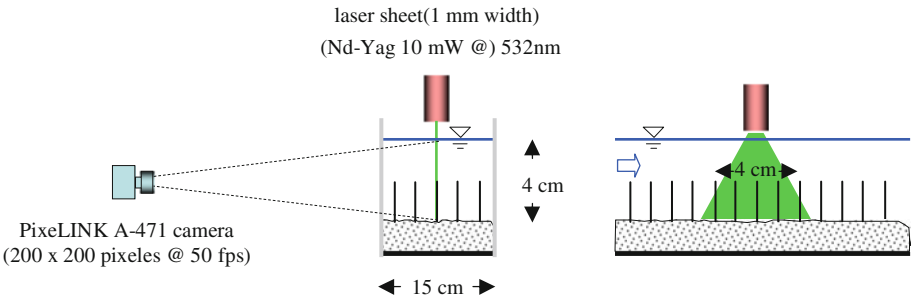

Fig. 3 Schematic disposition of the camera and the laser sheet source for PIV in the test section of the channel (not drawn to scale)

For water, Eq. 9 gives $u_\infty \simeq 10^{-5}$ cm/s. Even for flow velocities of about 1 cm/s the final velocity criterion is widely satisfied.

To apply this technique should be taken into account simultaneously the constraints arising from the geometry and dimensions of the flow under study, the characteristics of the technique, and limitations of available equipment:

- preliminary measurements with floats showed that the maximum speed on the free surface would be about of 12.0 cm/s for $\bar{U} = 6.0$ cm/s,
- shooting speed of 50 frames per second (fps) secured an acceptable tracer particle density,
- providing this shooting speed and with tracers moving close to the maximum flow velocity, they will travel a distance of about 2 mm, and given the need for a minimal amount of tracers (typically 5–10) remaining within interrogation window between consecutive frames, this meant that the length of these windows in the direction of flow should be about of 4 mm at least,
- pictures with a region of interest size of 200 × 200 pixels were able to capture details of the flow between the stems while preserving the definition of tracer particles,
- therefore, the measured region was 400 mm^2 and the volume of interrogation windows (32 × 32 pixels) was 6 × 6 × 1 mm^3.

The tracer particles were seeded slowly into the flow, in the vicinity of the bed, approximately 1.0 m upstream of the test section. The films were recorded in.avi format and stocked in .tiff format by using ImageJ (www.nih.com/ImageJ). Each film consisted of 250 frames equally spaced in time $\Delta t = 0.02$ s. This amount of frames rises from the compromise between the need for temporal averaging to extract reliable values of average velocity of the turbulent flow, and computational cost in the processing of all films. The processing of the recorded movies was performed using the free software URAPIV [32], which is based on cross-correlation with sub-pixel interpolation of each consecutive pair of frames. With an overlap of 75% it was possible to obtain measurements over six longitudinal stations within the PIV cell, see Fig. 4. The software output consists of 250 files.txt with the temporal evolution of the entire flow field in the plane shot.

Figure 5 presents frames extracted from the recorded movies, for the flow in the central vertical plane of the channel. Note the flat granular bed at the bottom, the stems as regular vertical shadows and the flat free surface of the flow at the top. The tracer particles were injected in the flow upstream enough to avoid perturbating the measurements. Due to turbulent mixing the tracers quickly occupy the entire bulk of the flow. As a consequence it was necessary to inject a big amount of tracers particles to have the desired density for obtaining quality images.

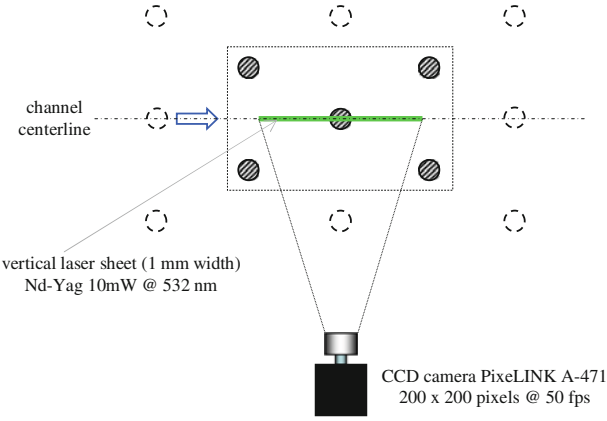

Fig. 4 Scheme of the elemental PIV cell covering the flow upstream and downstream of a central stem, as representative of the complete longitudinal region of flow variation between two consecutive stems of the array

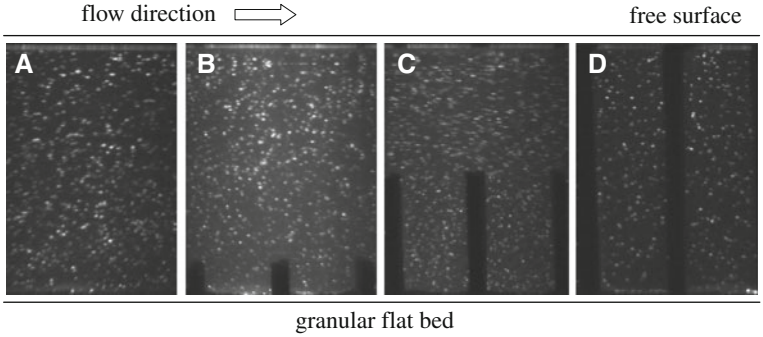

Fig. 5 Frames extracted from the recorded movies, for different relative submergences, for the flow in the central vertical plane of the channel: **a** flow over the granular bed without stems, **b** flow over the granular bed with stems of $h_v = 0.5\,\text{cm}$, **c** $h_v = 2.0\,\text{cm}$, and **d** $h_v = 4.0\,\text{cm}$

5 Results and discussion

5.1 Time-average velocity profiles

Following the Reynolds decomposition framework, the instantaneous Cartesian components for the velocity flow field can be expressed as:

$$\mathbf{u} = \mathbf{U} + \mathbf{u}' \tag{10}$$

where $\mathbf{U} = (U, V, W)$ is the time-average velocity field over a representative time span, and $\mathbf{u}' = (u', v', w')$ is the fluctuating component of the velocity field with zero time-average value, on identical time interval. The analysis begins with plots for the longitudinal and vertical velocity profiles, U and W, along the vertical coordinate, z, obtained from the PIV raw measurements.

Let us consider, in first place, the non-vegetated flow configuration, whose velocity profiles are shown in Fig. 6. The horizontal bars represent the value of the root mean square

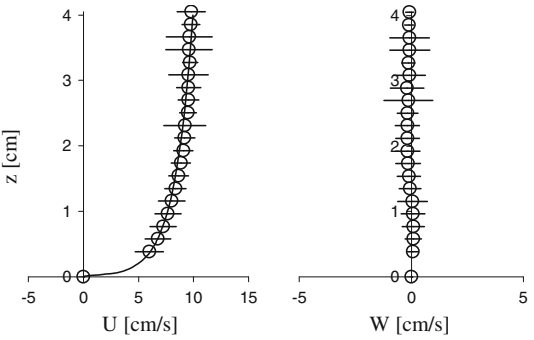

Fig. 6 Vertical U and W time-average velocity profiles, for a mean flow $\bar{U} = 6.0\,\text{cm/s}$ with $h = 4.0\,\text{cm}$, over a granular bed without rigid stems. The *solid line* corresponds to the fitted logarithmic velocity profile ($R^2 = 0.99$) for a uniform fully developed turbulent flow, with $u_* = 0.7\,\text{cm/s}$ and $z_0 = 0.01\,\text{cm}$. *Horizontal bars* represents the corresponding root mean square associated with the mean value, obtained from the PIV raw data

corresponding to each point, calculated from the PIV raw data. These results quantify the deviation from the mean value due to turbulent fluctuations in the flow field. From this point of view it is a useful tool to identify which areas of the flow field are more disturbed. They will also provide an effective and direct comparison between different flow configurations. As can be seen, close to the bed U quickly increases and reaches its maximum at the free surface. The continuous line corresponds to a fitted logarithmic profile for an uniform fully developed turbulent flow with $u_* = 0.7\,\text{cm/s}$ and $z_0 = 0.01\,\text{cm}$. The close-to-zero W values for all z imply a mainly longitudinal open channel flow, as can be expected in this configuration. As shown in Fig. 6, the turbulent fluctuations around the mean are roughly of the same magnitude throughout the flow depth.

Now, let us consider Fig. 7. This configuration corresponds to stems of $h_v = 0.5\,\text{cm}$, i. e., a case of well submerged vegetation. In first place, it is noticeable that the structure of the profiles has changed and shows remarkable differences when compared with the non-vegetated configuration. Roughly speaking, the time-average velocity profile U can be divided into two main regions: the vegetated layer for $0 \leq z < h_v$ and the free flow layer for $h_v < z \leq h$. It is seen that in the vegetated layer the flow becomes spatially dependent on the longitudinal coordinate, x, with U being lower downstream than upstream of the stem. For both profiles the values for U are less than the measured in the configuration without stems. This is a direct evidence of the resistance imposed by the stems on the flow. This deceleration effect due to the stems drag disappears at the free flow layer where the mean velocity profiles becomes practically indistinguishable. The maximum value for U appears at the free surface and an inflection point, joining these two flow layers, can be observed at $z = h_v$ approximately. Again, measurements show negligible values for W in the entire flow depth. In second place, the plots show an increment of the turbulent fluctuations around the mean values, U and W, with respect to the non-vegetated flow configuration shown in Fig. 6.

Following the analysis, Fig. 8 shows results for to the case of flow with submerged stems of height $h_v = 2.0\,\text{cm}$. As it can be seen, all the features of the previous case are present. The departure from the non-vegetated flow is more pronounced, with U reaching an almost constant value at short distance from the bed for the vegetated layer flow. It can be seen an inflection point in the profiles at $z \approx h_v$, and then a free flow layer developed over the tops of the stems. The flow is strongly decelerated by the stems drag and the spatial variability observed in the vegetated layer flow disappears for the free flow over the stems. The profiles

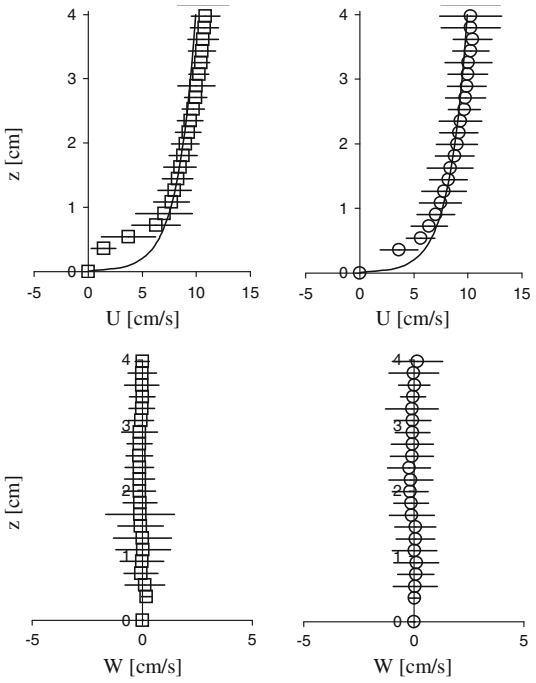

Fig. 7 Vertical U and W time-average velocity profiles, for a mean flow $\bar{U} = 6.0\,\text{cm/s}$ with $h = 4.0\,\text{cm}$, over a granular bed with rigid stems of $h_v = 0.5\,\text{cm}$. Markers are: *open square* time averaging immediately downstream the central stem, and *open circle* time averaging immediately upstream the central stem. The *solid line* corresponds to the fitted logarithmic velocity profile for nonvegetated uniform fully developed turbulent flow. *Horizontal bars* represents the corresponding root mean square associated with the mean value, obtained from the PIV raw data

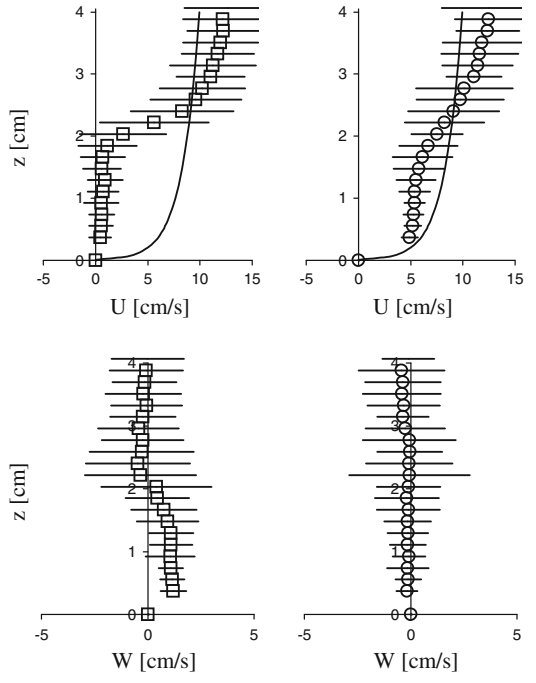

Fig. 8 Vertical U and W time-average velocity profiles, for a mean flow $\bar{U} = 6.0\,\text{cm/s}$ with $h = 4.0\,\text{cm}$, over a granular bed with rigid stems of $h_v = 2.0\,\text{cm}$. Markers are: *open square* time averaging immediately downstream the central stem, and *open circle* time averaging immediately upstream the central stem. The *solid line* corresponds to the fitted logarithmic velocity profile for nonvegetated uniform fully developed turbulent flow. *Horizontal bars* represents the corresponding root mean square associated with the mean value, obtained from the PIV raw data

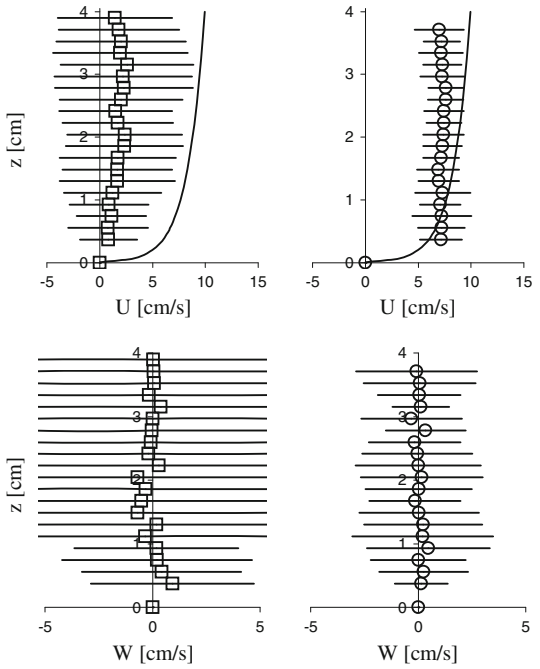

Fig. 9 Vertical U and W time-average velocity profiles, for a mean flow $\bar{U} = 6.0\,\text{cm/s}$ with $h = 4.0\,\text{cm}$, over a granular bed with rigid stems of $h_v = 4.0\,\text{cm}$. Markers are: *open square* time averaging immediately downstream the central stem, and *open circle* time averaging immediately upstream the central stem. The *solid line* corresponds to the fitted logarithmic velocity profile for nonvegetated uniform fully developed turbulent flow. *Horizontal bars* represents the corresponding root mean square associated with the mean value, obtained from the PIV raw data

for W suggest non negligible values for the flow immediately downstream a stem in the vegetated layer flow. For the free flow layer above the stems W is negligible, characteristic of a purely longitudinal shear flow. As regards the fluctuations around the mean value, the horizontal bars confirm the tendency previously observed: the rigid vegetation introduces a level of flow disturbance greater than those observed in the flow in absence of stems, and also greater than the observed in the precedent configuration of well-submerged vegetation. The correlation between the region where the fluctuations reach a maximum and the height of the stems is clearly observed in the plots.

The case of the flow with emergent stems, $h_v = 4.0\,\text{cm}$, is presented in Fig. 9, where only the vegetated layer flow is present. As expected, the constant value for the longitudinal mean flow, U, is for almost the entire flow depth. It is observed the strong deceleration for U immediately behind a stem and across the entire flow depth due to the stem drag. The spatial variability for U profiles in the longitudinal direction is also clearly observed when one takes into account the U profile immediately after the next stem downstream. The large increase for the velocity fluctuations is evident, being W negligible for all z in this configuration.

5.2 Velocity fluctuations and turbulence intensity

The plots for the time-average velocity profiles presented in the previous section, with the root mean square at each point as a quantification of the fluctuations around the mean, give an immediate and valuable information about the substantial changes in the flow structure introduced by the rigid vegetation. But the vegetation influence on the fluctuating component itself is missed in this analysis. Because of its importance, in this section this point will be considered with detail.

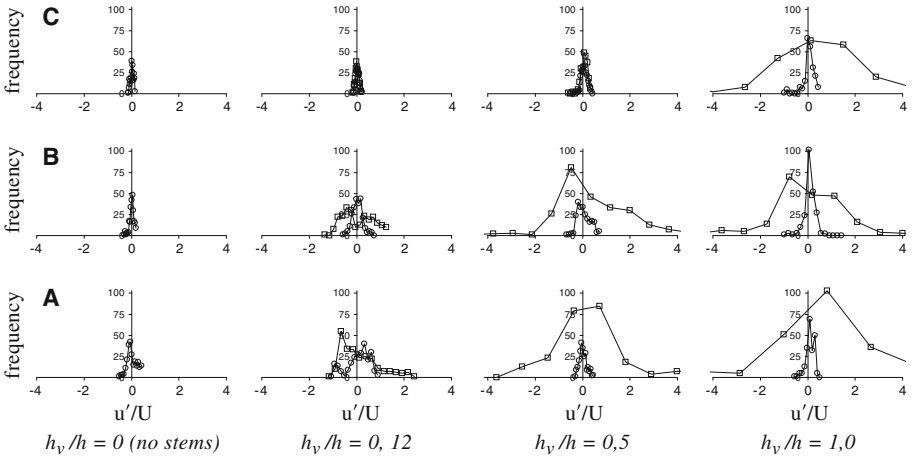

Fig. 10 Histograms for the relative fluctuations, u'/U for a mean flow $\bar{U} = 6.0\,\text{cm/s}$ with $h = 4.0\,\text{cm}$. Each row corresponds to three different heights from the bed: row **a** for $z = 0.35\,\text{cm}$, row **b** for z at the top of the stems (except for the case of non-vegetated flow, where it were considered measurements at the height $z = 2.0\,\text{cm}$), and row **c** for $z = 3.5\,\text{cm}$. The columns are organized with relative submergence from non-vegetated flow at the *left-hand side* to emergent stems flow at the *right-hand side*. Except for the case of flow without stems, markers are: *open square* 3 mm downstream of a stem, and *open circle* 3 mm upstream of a stem

The analysis will begin by considering plots showing the histograms, or frequency of occurrence diagrams, for the velocity field fluctuating component at specific points in the flow field. Based on the previous section, the analysis will be focused on the fluctuations for the predominant flow component, u'. Because of the spatial variations that have been observed, it can be hypothesized that u' will depend on the point along the flow field considered between two consecutive stems. For this reason, and to make these plots comparable for analysis, not only for different points in the same configuration but for analogous points in different configurations, it will be useful to present the histograms for u'/U, the relative fluctuation with respect to the mean at each point.

Row (A) in Fig. 10 shows four histograms for u'/U extracted from velocity measurements at $z = 0.35\,\text{cm}$ from the bed. From left to right h_v/h increases from 0 to 1. Except for non-vegetated flow, each plot shows two series of data: square markers corresponds to measurements at 3 mm downstream of a stem and circular markers for measurements at 3 mm upstream of a stem. Close to the granular bed, the tails of the histograms reveal an increase in the excursions for u'/U with h_v/h, being this fact more pronounced for the measurements behind a stem.

Row (B) in Fig. 10 presents histograms for u'/U at the top of the stems (except for the case of non-vegetated and emergent flow configurations, where it were considered measurements at the height $z = 2.0\,\text{cm}$ from the bed). The same features already noted for the plot at the row (A) are observed, indicating that the structure of relative fluctuations is maintained throughout the depth of the vegetated layer.

Finally, row (C) presents the histograms for u'/U at $z = 3.5\,\text{cm}$. It can be seen that the histograms of the measurements made downstream and upstream of the stems overlap. This is not the case for emerging stems, where the shape of the histograms resembles those of the previous cases. It is also observed a progressive increase of u'/U with h_v/h.

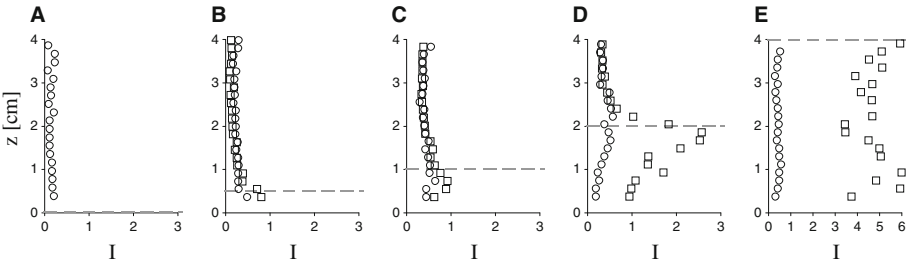

Fig. 11 Vertical profiles for the flow turbulence intensity, I, for a mean flow $\bar{U} = 6.0$ cm/s with $h = 4.0$ cm: **a** granular bed without rigid stems, **b** granular bed in presence of rigid stems with $h_v = 0.5$ cm, **c** $h_v = 1.0$ cm, **d** $h_v = 2.0$ cm, and **e** $h_v = 4.0$ cm. Except for the plot **a** (flow without stems), markers are: *open square* immediately downstream a single stem, and *open circle* immediately upstream

The histograms of u'/U give a good picture of the main sources of flow disturbance and their extreme values. In order to get more quantitative information, let us consider now the profiles for the flow turbulence intensity, or flow turbulence level, defined as:

$$I = \frac{\sqrt{rms(u')^2 + rms(w')^2}}{\sqrt{U^2 + W^2}} \tag{11}$$

Figure 11 shows several plots of I against z for the two locations under consideration (upstream and downstream a stem).

The analysis begins considering the case of flow in absence of stems. Figure 11a shows that I is roughly constant along the entire flow depth.

Figure 11b, for $h_v = 0.5$ cm, shows the changes in the structure of the flow turbulence: rigid vegetation introduces spatial variations in the I versus z profiles within the vegetated layer, where a remarkable increment of I is observed, with a maximum close to the top of the stems. At short distance above the stems, within the non-vegetated layer, I reaches a constant value with z, and there is no distinction between upstream and downstream measurements.

In Fig. 11c and d, for $h_v = 1.0$ cm and $h_v = 2.0$ cm, respectively, the trend previously observed is reinforced. In addition, the constant value of I outside the vegetation layer is larger than those of previous cases. Note that the maximum turbulence intensity occurs at the top of the stem. This feature is evident in Fig. 11d. Within the vegetated layer larger values of I downstream a stem implies larger excursions of the fluctuating component with small mean flow values.

Finally, in Fig. 11e, for emergent vegetation, the turbulence level is almost homogeneous along the entire flow depth with enhanced values, mainly downstream a stem (note that the plot scale is twice that in previous).

From these results it is concluded that the relative turbulence intensity in presence of vegetation is larger than the corresponding to non-vegetated conditions. In addition, the shape of the I profiles depends on the relative position to a stem, with the maximum values of I strongly dependent on h_v/h.

5.3 Double-averaged longitudinal velocity profiles.

Nikora [8] and Manes [9] have pointed out the relevance of spatially-averaged velocity profiles calculated from time-averaged profiles when studying flows in the presence of large scale roughness. The velocity profiles, $\langle U \rangle(z)$ in Fig. 12, represent longitudinal averages across

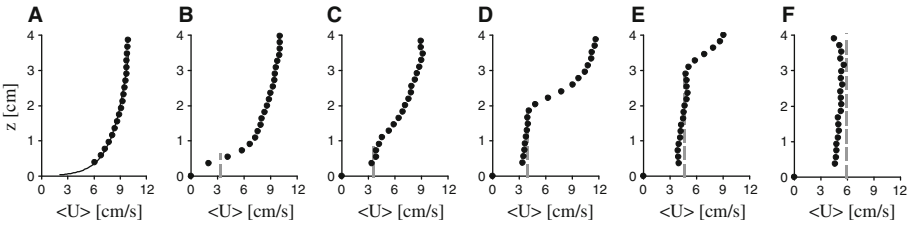

Fig. 12 Double-average velocity profiles, $\langle U \rangle(z)$, for the longitudinal component of the velocity field, u, for a mean flow $\bar{U} = 6.0\,\text{cm/s}$ with $h = 4.0\,\text{cm}$: **a** granular bed without rigid vegetation, **b** granular bed in presence of rigid stems with $h_v = 0.5\,\text{cm}$, **c** $h_v = 1.0\,\text{cm}$, **d** $h_v = 2.0\,\text{cm}$, **e** $h_v = 2.8\,\text{cm}$, and **f** $h_v = 4.0\,\text{cm}$. *Vertical dashed gray line*: uniform velocity predicted by Eq. 7 in the vegetated layer flow of height h_v

the six vertical profiles measured in the PIV cell, $U(z)$, as it has been previously explained in the Sect. 3.

As in the previous figures, Fig. 12a shows, at the left hand side, the velocity profile for the non-vegetated flow configuration, used as a reference case for comparison. The continuous line corresponds to the fitted logarithmic profile with $u_* = 0.7\,\text{cm/s}$ and $z_0 = 0.01\,\text{cm}$.

In Fig. 12b, for $h_v = 0.5\,\text{cm}$, is clear the influence of the rigid stems slowing down the flow and changing the shape of the velocity profile even if this represents a case of well-submerged vegetation with $h_v/h \ll 1$. The double-layer structure of the flow can be observed, joined by an inflection point at $z \approx h_v$.

The features observed in Fig. 12b are also present in Fig. 12c, for $h_v = 1.0\,\text{cm}$. Here, the influence of the stems drag over the flow is even more evident in the development of a nearly flat velocity profile within the vegetated layer. The flat portion of the profile occupies an increasing fraction of the total depth, h, as h_v increases, as shown in Fig. 12d and e, for $h_v = 2.0\,\text{cm}$ and $h_v = 2.8\,\text{cm}$, respectively.

Finally, a change on the mean flow velocity profile structure is observed when the flow through emergent stems is considered, $h_v = 4.0\,\text{cm}$, as shown in Fig. 12f. The constant value for the velocity profile is present in almost the whole flow depth, because of the disappearance of the upper layer free flow.

The vertical dashed gray line, of height h_v, that can be visualized in the plots of Fig. 12, represents the uniform velocity U_v predicted by the Eq. 7. It follows directly from the plots that U_v closely agrees with the height-average value of $\langle U \rangle(z)$ for $0 \leq z \leq h_v$. It is concluded that U_v constitutes an appropriate velocity scale for the flow inside the vegetated layer.

To inquire more deeply into these features, additional measurements were performed in the horizontal plane at $h_v/2$ from the bed, in the 5.0 cm long central third of the channel width, by changing the relative orthogonal positions of the PIV laser-camera arrangement. The objective was to explore the structure of the mean flow in the wake region behind the cylinders. The mean flow was set as in previous measurements, $\bar{U} = 6.0\,\text{cm/s}$ and $h = 4.0\,\text{cm}$.

Two series of three plots can be observed in Fig. 13. The (A) series corresponds to the spatially-averaged longitudinal flow in presence of submerged stems of $h_v = 1.5\,\text{cm}$: (A1) downstream a line of four stems, (A2) downstream a line of three stems, and (A3) in the PIV elementary cell previously defined, see Fig. 4. The (B) series correspond to analogous locations for the flow in presence of emergent stems, $h_v = 4.0\,\text{cm}$.

There are a number of features that can be analyzed from these plots. First of all, the stems drag is clearly visualized behind each row as a defect in the mean flow velocity. Moreover, it is clearly observed the correlation between the stem position and the minimum in velocity, with the maximum value located in between two lateral consecutive stems. In second term,

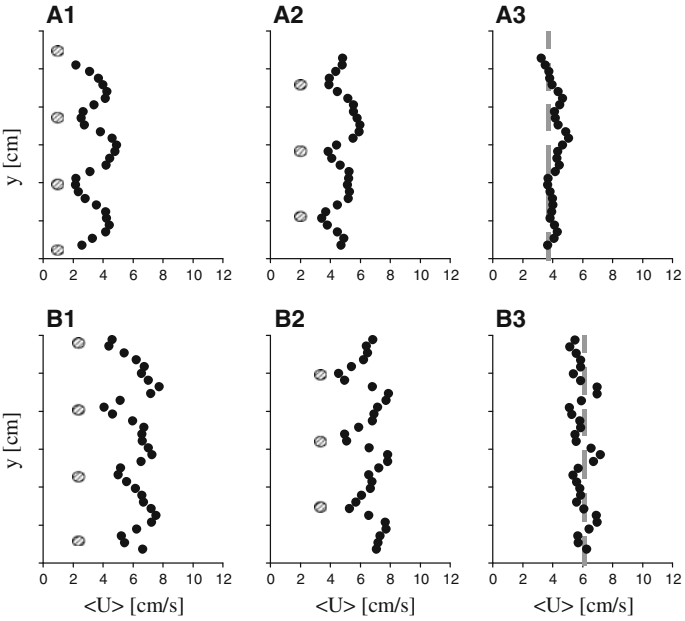

Fig. 13 Horizontal double-average velocity profiles, for the longitudinal velocity component, u, at the height $h_v/2$ from the bed, for a mean flow $\bar{U} = 6.0\,\text{cm/s}$ with $h = 4.0\,\text{cm}$. The **a** series in the upper row correspond to submerged stems, $h_v = 1.5\,\text{cm}$: **a1** downstream four stems, **a2** downstream three stems, and **a3** in the PIV elementary cell. The **b** series in the lower row correspond to emergent stems, $h_v = 4.0\,\text{cm}$: **b1** downstream four stems, **b2** downstream three stems, and **b3** in the PIV elementary cell. The *dashed gray line* corresponds to the velocity U_v predicted by the Eq. 7 for the uniform flow within the vegetated layer of height h_v

it can be seen that, in the flow direction, maximum velocity values behind a stem line are aligned with the minimum in the consecutive line downstream. Finally, when the spatial averaging over the complete PIV cell is carried out, see plots (A3) and (B3) in the Fig. 13, the close-to-constant value for $\langle U \rangle$ is again in good agreement with the prediction of Eq. 7.

5.4 Implications for the transport of solids, nutrients and contaminants.

The transport of sediment, nutrients and contaminants is an active field of research [33–36]. The published works mainly deal with flows over granular beds in absence of vegetation. In general, the sedimentary grains, tracers and particles are subject to the action of the instantaneous hydrodynamic forces due to the turbulent flow. The bed shear stress mean value (from double-averaged velocity profiles) is the usual first approach to the problem of quantifying critical values for initiation of sediment motion as bed load, and effective sediment transport conditions.

In the case of flow in presence of rigid vegetation, the results discussed above have shown several differences with an non-vegetated flow. The flow deceleration inside the vegetated layer suggests a protective role of the stems array, suggesting that an increased flow will be necessary to initiate sediment motion. This is in agreement with the results published by Jordanova and James [37] for experiments of sediment transport in presence of an array of emergent cylindrical vegetation with $\lambda_S = 0.03$ and $\lambda_K = 0.32$. The results presented

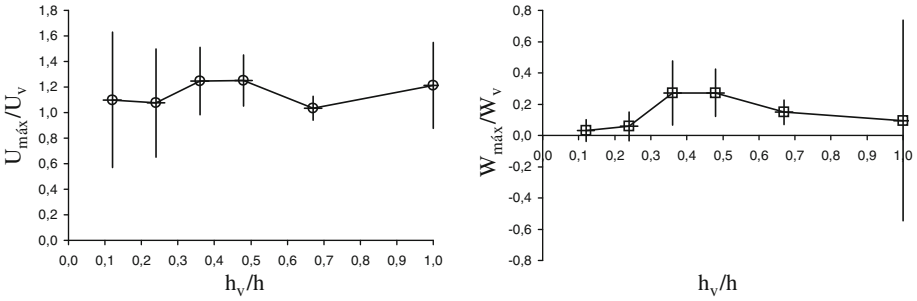

Fig. 14 Variation of the maximum values measured for U and W, relative to U_v, with h_v/h, extracted from measurements close to the granular bed (3.5 mm)

here indicate that a proper modeling of the critical and effective transport conditions must incorporate the features observed in vegetated flows. It should be taken into account that, depending on h_v/h, there are zones between the stems and close to the sedimentary bed where U reaches larger values than U_v. Moreover, in the range $0.3 \leq h_v/h \leq 0.6$ the measurements suggest a very complex flow-stems interaction close to the bed, because of the non-negligible time-average vertical velocities observed downstream a stem. On the other hand, turbulent intensity levels measured in the presence of rigid stems were always higher than those observed in their absence. Also, the structure of relative turbulent intensity profiles were more complex than that observed in the flow without vegetation. All these findings are summarized in Fig. 14, showing the dependence with h_v/h for the maximum U and W values, relative to U_v and extracted from the measurements at 3.5 mm from the granular bed. The vertical bars, obtained from the root mean square of the flow fluctuating components, show the wide range of variation that can be reached by U and W, with values as far as 1.6 in the case of U_{max}/U_v.

6 Conclusions and perspectives

The present contribution presents PIV measurements for the flow field in a horizontal small open channel over a rough bed of glass beads in presence of an array of staggered rigid stems. The objective was to explore the influence of the stems-to-flow relative submergence, h_v/h, on the structure of a stationary uniform fully developed flow for a constant channel Reynolds number, $Re = 6,300$. Measurements over the same rough bed in absence of stems allow a direct comparison between vegetated and non-vegetated flows.

The measurements have shown a strong influence of h_v/h on the longitudinal time-average and double-averaged velocity profiles, velocity fluctuations and intensity of the flow turbulence.

The deceleration of the flow due to the hydrodynamic resistance of the stems array is remarkable in a layer of height approximately equal to h_v even in the case of small h_v/h values (well submerged vegetation).

The time-averaged velocity profiles for positions between two consecutive stems reveal a predominantly longitudinal flow highly spatially-dependent inside the vegetated layer of height h_v. For submerged stems this spatial variation is no longer appreciable in the layer of the flow ranging from a short distance above the top of the stems to the free surface, where the maximum velocities occur. But it is noticeable that any effort to adjust a theoretical velocity profile for this upper flow layer must deal with the problem of finding an adequate scale

velocity at the bottom of this profile (i. e., on the top of the stems) where the structure of the longitudinal flow is far to have a unique description due to the observed spatial variation at $z = h_v$.

The relative velocity fluctuations and turbulence intensities are larger when compared with the non-vegetated flow, even close to the granular bed. These increased values depend on h_v/h and on the position along the flow between two consecutive stems, with maximum values occurring below but very close to the top and immediately downstream to a given stem.

The double-averaged longitudinal velocity profile reveals a characteristic structure: it grows quickly from the bed and reaches a constant value that is extended over the vegetation height, h_v. Then an inflection point is always visible at $z \approx h_v$, and finally a layer of free flow over the stems develops reaching the free surface where maximum velocity occurs. For emergent stems there is no inflection point, and the flat structure for the velocity profile extends up to the free surface. The comparison between the close-to-flat double-averaged profile for the longitudinal flow inside the vegetated layer with the prediction of the Eq. 7 for the height averaged mean flow in this layer shows a close agreement. This fact indicates that U_v is a reliable velocity scale for the height-average mean flow inside the vegetated layer.

The modified turbulent structure of the flow, with larger turbulent fluctuations close to the bed and with intensities depending on both h_v/h and the position between stems, should be taken into account when modelling the forces over particles (sediment, nutrients and contaminants), due to the destabilizing role of flow turbulence on granular material [33,36]. Turbulence intensity profiles show a complex distribution in the vegetated flow, especially with submerged stems. All these findings are indicative that more than one longitudinal balance of mean hydrodynamic forces will be necessary for a proper characterization of the sediment-flow interaction when vegetation is present.

References

1. Järvelä J (2006) Flow sediment vegetation interaction: research challenges, river flow 2006. Taylor and Francis Group, London
2. Salvia M (2009) Estimating flow resistance of wetlands using SAR images and interaction models. Remote Sens 1:992–1008
3. Major sediment issues confronting the Bureau of Reclamation and Research Needs Towards Resolving These Issues, Proceedings of the U.S. Geological Survey (USGS) Sediment Workshop (1997) In: Yang CT, Young, CA (eds) U.S. Bureau of Reclamation: Riparian vegetation and its effect on bed roughness and controlling channel width and soil erosion. It is necessary to quantify the effects of friction losses in flows through flexible and rigid vegetation. What are the effects of vegetation to bank erosion rates and to the onset of sediment transport? Harpers Ferry, West Virginia, US
4. Le Hir P (2007) Sediment erodability in sediment transport modelling: Can we account for biota effects? Cont Shelf Res 27:1116–1142
5. López F (2001) Mean flow and turbulence structure of open-channel flow through non-emergent vegetation. J Hydraul Eng 127(5):392–402
6. Neary VS (2003) Numerical solution of fully developed flow with vegetative resistance. J Hydraul Eng 129(5):558–563
7. Yen BC (2002) Open channel flow resistance. J Hydraul Eng 128(1):20–39
8. Nikora V (2004) Velocity distribution in the roughness layer of rough-bed flows. J Hydraul Eng 130(10):1036–1042
9. Manes C (2007) Double-averaged open-channel flows with small relative submergence. J Hydraul Eng 133(8):896–904
10. Stone BM, Shen HT (2002) Hydraulic resistance of flow in channels with cylindrical roughness. J Hydraul Eng 128(5):500–506
11. Carollo FG (2002) Flow velocity measurements in vegetated channels. J Hydraul Eng 128(7):664–673

12. Poggi D (2004) The effect of vegetation density on canopy sub-layer turbulence. Bound Layer Meteorol 111(6):565–587
13. Huthoff F (2007) Analytical solution of the depth-averaged flow velocity in case of submerged rigid cylindrical vegetation. Water Resour Res 43:W06413
14. Baptist MJ (2007) On inducing equations for vegetation resistance. J Hydraul Res 45(4):435–450
15. Nepf HM (2000) Flow structure in depth-limited, vegetated flow. J Geophys Res 105(12):28547–28557
16. Nepf HM (2006) The structure of the shear layer in flows over rigid and flexible canopies. Environ Fluid Mech 6:277–301
17. Klopstra D (1997) Analytical model for hydraulic roughness of submerged vegetation, 27th Congress of the International Association for Hydraulic Research, San Francisco, California, US, pp 775–780. ASCE, ISBN 90-77051-03-1
18. Garcia MH (2004) Flow, turbulence and resistance in a flume with simulated vegetation, Riparian vegetation and fluvial geomorphology. In: Bennet SJ, Simon A (eds) Water science and application 8. AGU, Washington
19. White FM (1979) Mecánica de Fluidos, 652. McGraw-Hill, México
20. Raffel M, Willert C, Kompenhans J (2000) Particle image velocimetry: a practical guide. Springer-Verlag, Berlin
21. Adrian RJ (1997) Dynamic ranges of velocity and spatial resolution of particle image velocimetry. Meas Sci Technol 8:1393–1398
22. Adrian RJ (2004) Twenty years of paricle image velocimetry, 12th International symposium on applications of laser techniques to fluid mechanics. Lisbon, Portugal
23. Olsen MG (2001) Measurement volume defined by peak-finding algorithms in cross-correlation particle image velocimetry. Meas Sci Technol 12:14–16
24. Prasad A (2000) Particle image velocimetry. Curr Sci 79(1):51–60
25. Westerweel J (1997) Fundamentals of digital particle image velocimetry. Meas Sci Technol 8:1379–1392
26. Melling A (1997) Tracer particles and seeding for particle image velocimetry. Meas Sci Technol 8:1406–1416
27. Stanislas M (1997) Practical aspects of image recording in particle image velocimetry. Meas Sci Technol 8:1417–1426
28. Huang H (1997) On errors of digital particle image velocimetry. Meas Sci Technol 8:1427–1440
29. Nogueira J (1997) Data validation, false vectors correction and derived magnitudes calculation on PIV data. Meas Sci Technol 8:1493–1501
30. Jakobsen ML (1997) Particle image velocimetry for predictions of acceleration fields and force within fluid flows. Meas Sci Technol 8:1502–1516
31. Acheson DJ (1990) Elementary fluid dynamics. Oxford University Press, Oxford
32. Gurka R (1999) Computation of pressure distribution using PIV velocity data, 3rd International workshop on particle image velocimetry, California
33. Zanke UCE (2003) On the influence of turbulence on the initiation of sediment motion. Int J Sediment Res 18(1):17–31
34. Dey S (2008) Sediment threshold under stream flow: a state-of-the-art review. Water Eng 12(1):45–60
35. Coleman SE (2008) A unifying framework for particle entrainment. Water Resour Res 44, W04415 1-10
36. Valyrakis M (2010) Role of instantaneous force magnitude and duration on particle entrainment. J Geophys Res 115, F02006 1-18
37. Jordanova AA, James CS (2003) Experimental study of bed load transport through emergent vegetation. J Hydraul Eng 129(6):474–478
38. Meijer DG, Van Velzen EH (1999) Prototype-scale flume experiments on hydraulic roughness of submerged vegetation. 28th IAHR Congress (1999), Graz, Austria